Chemical Papers
https://doi.org/10.1007/s11696-020-01200-7

ORIGINAL PAPER

Synthesis and characterization of a novel non-symmetrical bidentate Schiff base ligand and its Ni(II) complex: electrochemical and antioxidant studies

Imène Bougossa[1] · Djouhra Aggoun[1,2] · Ali Ourari[1] · Raúl Berenguer[3] · Sofiane Bouacida[4] · Emilia Morallon[3]

Received: 5 November 2019 / Accepted: 15 May 2020

Abstract

This paper describes the synthesis and properties of a new nitro-substituted bidentate Schiff base ligand (**HL**) and its nickel complex (**Ni(II)-2L**). Its ligand was derived from the condensation of 2′-methoxyphenyl-2-ethylamine with 5-nitro-2-hydroxybenzaldehyde. This ligand and its nickel complex were characterized through *elemental analysis*, UV–Vis, IR, ^{1}H NMR and ^{13}C NMR. The molecular structure of the nickel complex was confirmed using single-crystal X-ray diffraction. This complex crystallizes in dichloromethane in triclinic system, space group of P-1 with $a = 6.6803$ (2), $b = 9.6702$ (2), $c = 12.1836$ (3) and 1 formula unit in the cell. The obtained data revealed that the Ni(II) center is tetra-coordinated by two oxygen and two nitrogen atoms involving two ligands. Cyclic voltammograms of the nickel complex, recorded in DMF solutions, showed one quasi-reversible redox couple related to the Ni(II)/Ni(I) couple, demonstrating its electro-activity. This indicates a slow redox transition and/or electron exchange process, which implies that this electrochemical process is mainly diffusion-controlled. The antioxidant activity of the synthesized compounds was evaluated from the reactivity with the free radical DPPH, showing IC_{50} values between 0.4 and 4.5 mg/mL.

✉ Djouhra Aggoun
aggoun81@yahoo.fr

[1] Laboratoire d'Electrochimie, d'Ingénierie Moléculaire et de Catalyse Rédox (LEIMCR), Département Génie des Procédés, Faculté de Technologie, Université Ferhat ABBAS Sétif-1, 19000 Sétif, Algeria

[2] Département de Chimie, Faculté des Sciences, Université Ferhat ABBAS Sétif-1, 19000 Sétif, Algeria

[3] Departamento de Química Física, Instituto Universitario de Materiales, Universidad de Alicante (UA), Ap. 99, 03080 Alicante, Spain

[4] Département Sciences de la Matière, Faculté des Sciences Exactes et Sciences de la Nature et de la Vie, Université Oum El Bouaghi, Oum El Bouaghi, Algeria

Graphic abstract

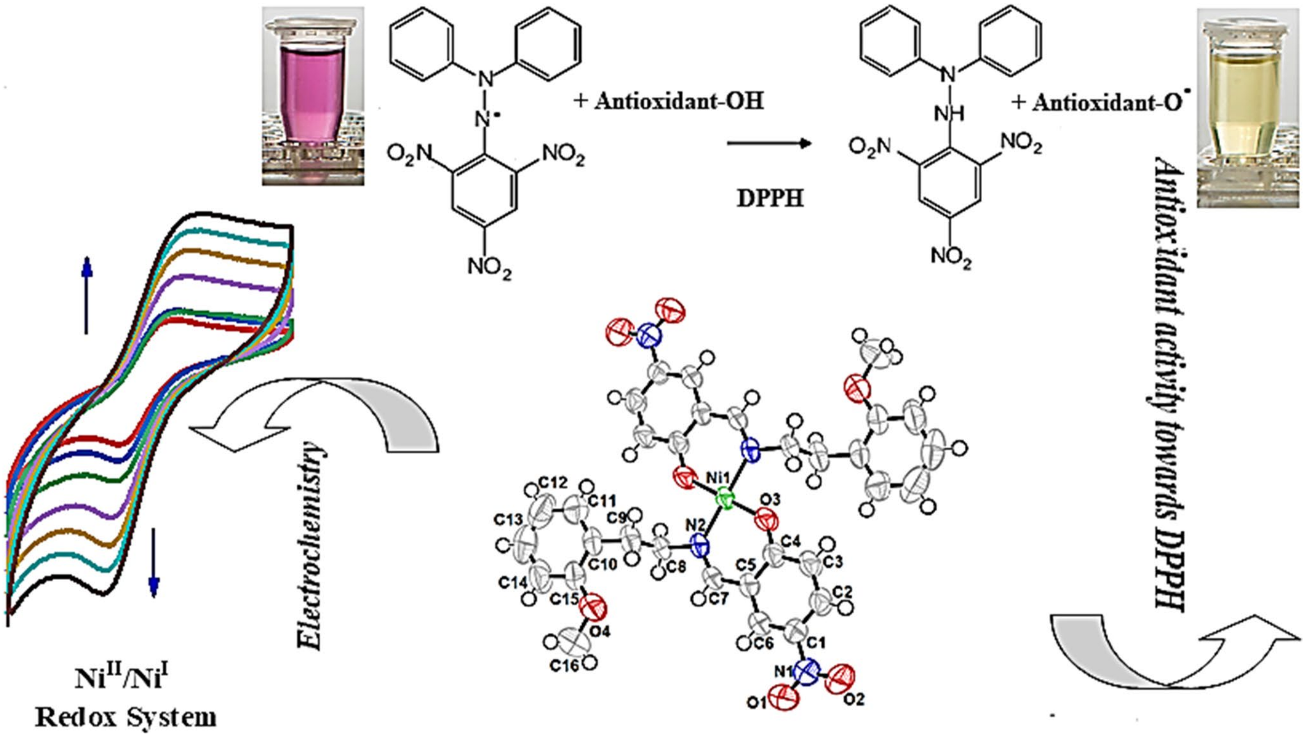

Keywords Bidentate Schiff base · Nickel(II) complex · X-ray diffraction · Electrochemical reduction · Antioxidant activity

Introduction

Obtained by condensation of aldehydes with primary amines, Schiff bases are versatile ligands in the field of coordination chemistry currently containing nitrogen, oxygen and other donor atoms (Djebbar et al. 1997; Tai et al. 2003; Wu et al. 2001; Bhattacharya et al. 1998), able to be applied in a wide range of applications (Gungor and Kara 2011; Yahsi et al. 2011; Hopa et al. 2010; Odabasioglu et al. 2009; Kara and Naturforsch 2008; Dey et al. 2003; Amirnasr et al. 2001; Chang et al. 2016; Dey et al. 2002; Nassimbeni et al. 1976).

In parallel, considerable interest has aroused in the comparative donor properties of oxygen and nitrogen when both are present in the same molecule (Al-allaf and Sheet 1995). In fact, many organic ligands containing these donor atoms have been systematically studied in recent years with very successful results in the synthesis of high nuclearity of complexes. This may be attributed to their relative high stability, biological activity (Highfield et al. 2000; Das et al. 1999) and potential applications in many fields such as oxidation catalysis (Djebbar et al. 1998), electrochemistry (Gorczyński et al. 2016) and analytical chemistry (Dalia et al. 2018; Altun et al. 2009). Hence, the design of new Schiff base ligands containing N and O atoms or functional groups with electrodonor capability is then very interesting for metal complexation (Alturk et al. 2015). Particularly, the chemistry of nickel Schiff base complexes has been the subject of extensive investigation in the past decades (Kuchtanin et al. 2016). Many of these studies were essentially focused on the electrocatalytic reduction activity of the Schiff base complexes in a large number of homogeneous (Luca et al. 2012) and heterogeneous reactions (Bedioui et al. 1991). It was generally found that the nature of the ligand determines the properties of the complex, so the design and synthesis of novel ligands become a hot topic in this field. Among different types, the ortho-hydroxylated Schiff bases, incorporating another e-donating functionality, have received a special attention to build these new bidentate structures. Taking into account of these facts, a novel Schiff base ligand and its nickel(II) complex were synthesized and characterized using different spectroscopies and analytical methods, such as IR, ^{1}H NMR, ^{13}C NMR, UV–Vis. The crystal structure of the nickel(II) complex has also been determined using crystallographic studies. Electrochemical behavior of the nickel complex was investigated by cyclic voltammetry. Moreover, these compounds were found be endowed with antioxidant activity after testing them by the

DPPH (1,1-diphenyl-2-picrylhydrazyl) showing that IC_{50} values were also found to be between 0.5 and 4.0 mg/mL.

Experimental

Materials

All chemicals and solvents used in this work were obtained from commercial sources and were used as received without any further purification. The purity of the synthesized compounds was checked by means of thin-layer chromatography (TLC). In this analysis, glass plates precoated with silica gel (60F, Merck) were used.

Synthesis of the ligand and its Ni(II) complex

The synthesis of the bidentate Schiff base ligand and its Ni(II) complex is summarized in Scheme 1. Basically, 2-methoxyphenylethylamine (1 mmol, 151 mg) and 5-nitro-2-hydroxybenzaldehyde (1 mmol, 167 mg) were dissolved in absolute ethanol (16 mL). The mixture was refluxed for 3 h. A yellow precipitate was observed as soon as the first contacts have been took place, and the expected product was then recovered by filtration after its washing several times small portions of cold ethanol. To synthesize this complex, a solution of $Ni(OCOCH_3)_2{\cdot}4H_2O$ (0.5 mmol, 124 mg) in ethanol (8 mL) was added and mixed with the previous ethanolic solution of ligand. After contact of these two solutions, a green precipitate of the complex (**Ni(II)-2L**) was immediately observed and, then, the mixture was again refluxed for 4 h for completion of the reaction. The formed solid was again recovered by filtration and finally washed with small portions of cooled ethanol.

Physicochemical and electrochemical characterization

The uncorrected melting points of the ligand and its complex were measured with a Kofler Bench (model WME) apparatus. Elemental analysis (C, H and N) of the new compounds was carried out with the aid of a vario EL III elemental analyzer, whereas ^1H NMR and ^{13}C NMR spectra were recorded by using a 400 MHz Bruker NMR spectrometer and $CDCl_3$ as solvent. In this characterization, the chemical shifts (δ) were referenced to tetramethylsilane (TMS), used as internal reference and expressed in ppm. Infrared transmission spectra were obtained, after preparing KBr pellets using a Bruker IR instrument. UV–Vis spectra of the compounds were obtained in CH_2Cl_2 with the aid of an UNICAM UV-300 instrument.

The cyclic voltammograms were recorded a 10 ml cell equipped with three conventional electrodes containing DMF solutions and 0.1 M tetra-n-butylammonium perchlorate (TBAP) as supporting electrolyte. For the preparation of working electrodes, the compounds were supported on a rod of glassy carbon (3 mm diameter) previously polished by diamond paste and rinsed with acetone and then DMF. The counter electrode was a platinum wire, whereas a saturated calomel electrode (SCE) was used as the reference.

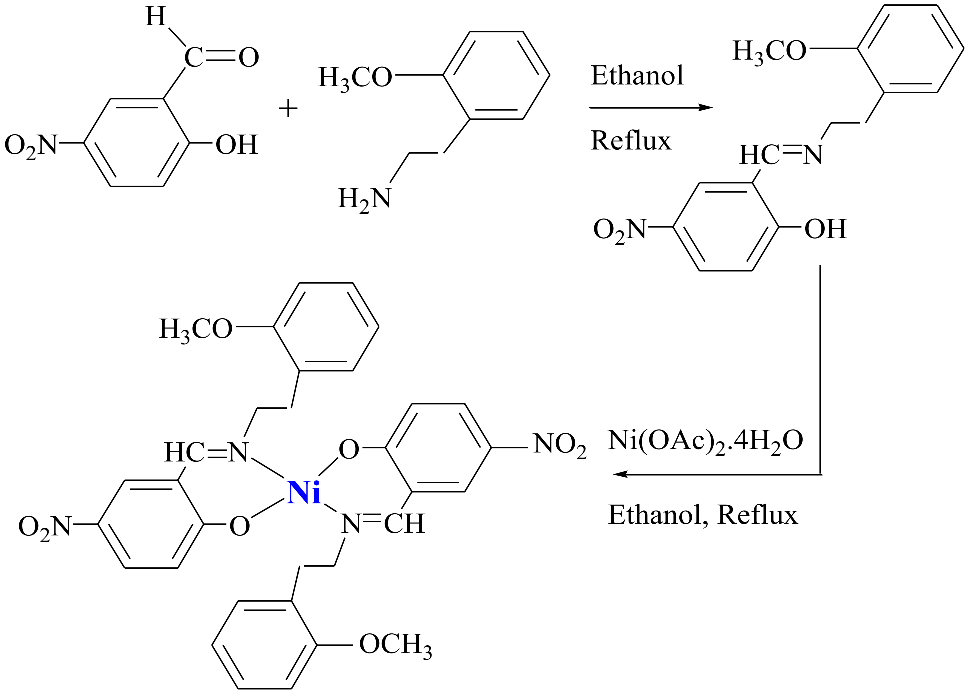

Scheme 1 Experimental procedure showing the synthesis of the bidentate Schiff base ligand (**HL**) and its nickel complex (**Ni(II)-2L**)

Zero-grade Ar (Air Products) was used to deaerate all electrolytic solutions.

X-ray crystallography

Green prismatic single crystals of the complex (**Ni(II)-2L**) were obtained after their redissolution followed by slow evaporation in/of dichloromethane. The crystal was coated with paratone® oil and mounted on loops for data collection. X-ray data were collected with a Bruker Apex II CCD area detector diffractometer by using a graphite monochromated Mo-Kα radiation source ($\lambda = 0.71073$ Å) at 150 K. The crystallographic data and experimental details for structural analysis are summarized in Table 3. The reported structure was solved by direct methods with SIR2004 (Burla et al. 2005) to locate all the non-H atoms, which were refined anisotropically with SHELXL97 (Sheldrick 2008) and using full-matrix least squares on F2 procedure from within the WINGX suite of software (Farrugia 2012) used to prepare material for publication. All the H atoms were placed in the calculated positions and constrained to ride on their parent atoms. Drawings of molecules were produced with the program ORTEP-3 and Diamond (Farrugia 1997; Brandenburg and Berndt 2001).

Antioxidant activity

The antioxidant activity, given as the ability of the synthesized compounds to scavenge hydrogen peroxide, was determined according the method described by the literature (Al Zoubi et al. 2016). For this analysis, an equal volume of each fraction of the both synthesized compounds was added to a methanolic solution of 2,2-diphenyl-1-picrylhydrazyl (DPPH) using different concentrations of this free radical. This mixture is vigorously shaken at room temperature during 30 min. The absorbance of the solution is then measured at 517 nm. The radical scavenging activity, expressed as the inhibition percentage, was calculated according the following relation:

$$\%\text{inhibition} = \frac{\left(\text{Abs}_{\text{control}} - \text{Abs}_{\text{test}}\right)}{\text{Abs}_{\text{control}}}$$

where $\text{Abs}_{\text{control}}$ and Abs_{test} are the absorbance of the standard (ascorbic acid) and the sample, respectively. The provided activity was given as the IC_{50} value (50% inhibitory concentration) in mg/mL.

Results and discussion

Physicochemical properties and molecular formulae

Some of the chemical and physical properties of the synthesized Schiff base ligand (**HL**) and Ni complex (**Ni(II)-2L)** are presented in Table 1. Both the ligand and its complex of nickel were stable at room temperature and were soluble in DMF, DMSO, ACN and dichloromethane. The retarding factors (R_f) were found to be 45 and 56, respectively, whereas their melting points are ranged between 100 and 200 °C. Elemental analysis of the ligand showed that it contains ca. 64% of carbon and almost 5 and 9% of hydrogen and nitrogen, respectively. This composition agrees perfectly with molecular formulae ($C_{16}H_{16}O_4N_2$) of the ligand. In the case of the complex, the C% was found to be practically the expected value whereas those of hydrogen and nitrogen showed very small differences that are practically acceptable. Therefore, its molecular formula is consistent with $C_{32}H_{30}O_8N_4Ni$.

IR spectra

The IR spectrum of the bidentate Schiff base ligand (**HL**) (Fig. 1) exhibits a broad absorption band, centered at around 3445 cm^{-1} that can be assigned to the O–H interactions like inter- and intramolecular hydrogen bonds. The free hydroxyl group is characterized by its own stretching vibration appearing at higher energy around 3700 cm^{-1} (Ebrahimi et al. 2014). The presence of an intense band at 1657 cm^{-1} was attributed to the stretching vibration of

Table 1 Physicochemical properties and proposed molecular formulae of the synthesized compounds

Compound	Color	R_f^a	Yield (%)^{b,c}	M.p. (C°)	Elemental analysis^d			Molecular formula
					C (%)	H (%)	N (%)	
HL	Yellow	45	70	106	64.18 (64.00)	5.41 (5.38)	8.81 (9.33)	$C_{16}H_{16}O_4N_2$
Ni(II)-2L	Green	56	25	194	58.46 (58.47)	4.69 (4.56)	8.02 (8.53)	$C_{32}H_{30}O_8N_4Ni$

[a] Retarding factor values obtained from mixture of dichloromethane/ethanol (9/0.5, v/v) as eluent

[b] Mole number of ligand/mole number of aldehyde

[c] Mole number of complex/mole number of ligand, M.p.: melting point

[d] Microanalysis C, H, N, found and (calculated) values

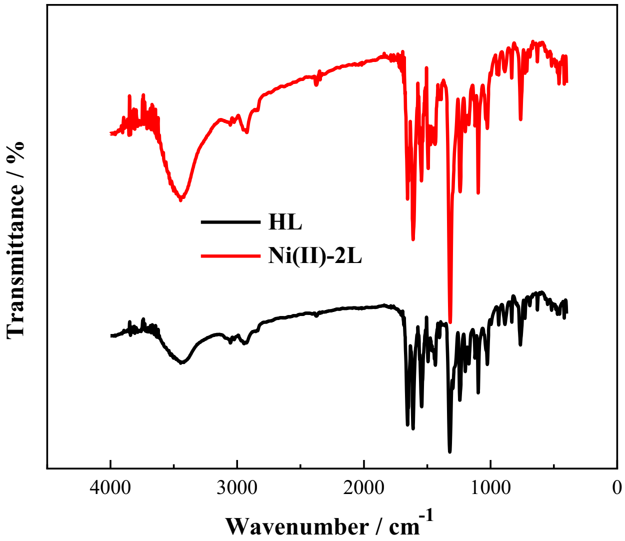

Fig. 1 IR spectra of the ligand (**HL**) and its nickel complex (**Ni(II)-2L**)

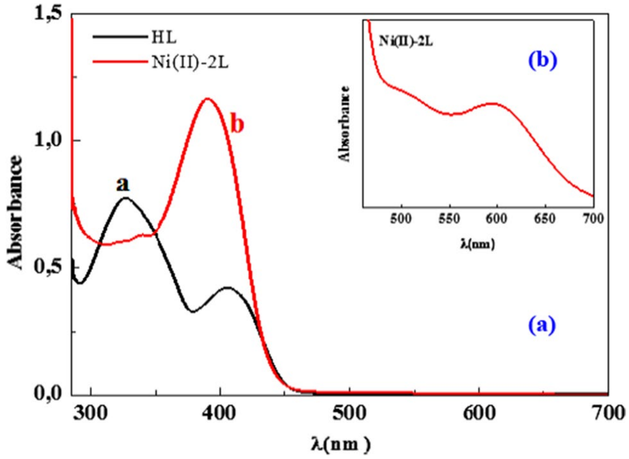

Fig. 2 UV-Vis spectra of 10^{-5} M CH_2Cl_2 solutions of **HL** (**a**) and **Ni(II)-2L** (**b**).The *inset* shows the MLCT and d-d transitions, recorded in the 450–700 nm region using 10^{-3} M solutions of the complex

the azomethine group (HC=N). This band is also present in the IR spectrum of the **Ni(II)-2L** complex (Fig. 1) but, in this case, it has been shifted to lower energy appearing at 1609 cm^{-1}. This shifting is explained by an extension of the electronic delocalization through the nickel center and the both azomethine groups (Ilhan et al. 2007). Furthermore, this Schiff base ligand displays also two other bands at around 1540 cm^{-1} and 1431 cm^{-1}, respectively. These absorption bands have been assigned to the ν_{asym} and ν_{sym} (NO_2) modes, respectively (Cisterna et al. 2015). The band located at 1305 cm^{-1} for the ligand **HL** is attributed to the phenolic ν (C–O) stretching vibration. This band is shifted to the higher frequencies (1317 cm^{-1}) in the spectrum of the nickel complex. This shifting suggests that the hydroxyl groups of the both Schiff base ligands have taken part in the formation of nickel complex. These observations suggest that the metallic ion was effectively coordinated to the four coordinating heteroatoms (NONO) (VimalKumar and Radhakrishnan 2011). Other conclusive absorption bands of this complex (**Ni(II)-2L**) were also observed between 420–480 and 500–650 cm^{-1}. These absorption bands were ascribed to the Ni–N and Ni–O stretching vibrations, respectively (El-Megharbel et al. 2016).

UV–Vis spectra

The UV–Vis spectrum of the ligand **HL** (Fig. 2) showed two intense absorption bands at 302 and 407 nm, respectively. The first band appears at higher energy with a strong intensity may be assigned to the $\pi-\pi^*$ electronic transition of the azomethine chromophore and the benzene ring. The second, being weaker band, is attributed to $n-\pi^*$ transition of the (C=N) azomethine group (Keypour et al. 2013; Ourari et al. 2014). This band is also present in the electronic spectrum of the complex **Ni(II)-2L** displaying small shifting to higher energy at 388 nm. This is due of the coordination of the nitrogen atom of the azomethine groups to the metal center. The electronic absorption spectrum of the complex shows a shoulder at 498 nm which could be assigned to the charge transfer between the metallic center and the coordinating atoms of the ligand (i.e. the so-called metal ligand charge transfer, MLCT) (Khalaji et al. 2011). The absorption bands of **Ni(II)-2L** complex observed at around 600 nm (see inset of Fig. 2), with its characteristic weaker intensities ($\varepsilon = 0.288.10^3$ mol^{-1} L cm^{-1}), are attributable to the d–d transitions (Pooyan et al. 2013).

^{1}H NMR and ^{13}C NMR spectra

^{1}H NMR and ^{13}C NMR spectral data of the Schiff base **HL**, and **Ni(II)-2L** complex are listed in Table 2. The ^{1}H NMR spectrum of the Schiff base ligand **HL** (Fig. 3a) shows a sharp singlet (s) at 8.12 ppm attributed to the azomethine proton (–HC=N–). The multiplet of the aromatic protons was observed in the range 6.80–7.30 ppm. The methylene group δ Ph–$CH_{2(8)}$ resonates at 3.05 ppm. As for the N–$CH_{2(9)}$, it absorbs at 3.87 ppm while the protons of the methoxy group (δCH_3O) slightly appear at stronger fields resonating at 3.81 ppm.

Regarding the ^{13}C NMR spectrum (Fig. 3b), the **HL** Schiff base ligand shows the azomethine carbon peak at 164.28 ppm. The Ph–$CH_{2(8)}$, N–$CH_{2(9)}$ and –$OCH_{3(1)}$ are detected at 31.76, 56.58 and 55.31 ppm, respectively, as illustrated in Fig. 3c. The aromatics carbons are observed in the expected region between 110 and 140 ppm. In the

Table 2 ^{1}H NMR and ^{13}C NMR spectral data of the Schiff base (HL) and its nickel complex (Ni(II)-2L) in $CDCl_3$

^{1}H NMR	**N=CH**	**N–CH$_{2(9)}$**	**Ph–CH$_{2(8)}$**	**–OCH$_{3(1)}$**	**H$_{(3\text{-}6,12\text{-}13\text{-}15)}$**
HL	8.12 (s,1H)	3.87 (t,2H)	3.05 (t,2H)	3.81 (s,3H)	7.30–6.80(m,7H)
Ni(II)-2L	8.07 (s,1H)	3.80 (t,2H)	3.10(t,2H)	4.30 (s,3H)	6.40–7.80(m, 7H)
^{13}C NMR	**N=C$_{(10)}$H**	**N–CH$_{2(9)}$**	**Ph–CH$_{2(8)}$**	**–OCH$_{3(1)}$**	**C$_{(2–7,\ 11–16)}$**
HL	164.28	56.58	31.76	55.31	100–140
Ni(II)-2L	157.76	64.31	29.25	55.45	100–140

Multiplicities of signals are singlet (s), triplet (t) and multiplet (m) with their chemical shifts expressed in ppm

^{13}C NMR spectra of the complex, all the carbons peaks are slightly shifted to the downfields when they are compared to those of the corresponding Schiff base ligand.

Description of crystal structure

Structural resolution revealed that the asymmetric unit of the complex consists of half molecule of **Ni(II)-2L** and the second half is generated by symmetry, the Ni atom is located at an inversion center (Figure 4). The nickel complex **Ni(II)-2L** crystallizes in dichloromethane in the triclinic crystal system with *P*-1 space group with 1 formula unit in the cell (Table 3). The ORTEP (Farrugia 2012) diagram of the titled compound is shown in Fig. 4.

The crystal structure of **Ni(II)-2L** was formed from two units of bidentate Schiff base ligand totalizing four dentate in its coordination sphere as it can be seen in Fig. 4. The nickel ion was found to be placed in a square-planar environment, currently adopted by this metal. This coordination was accomplished in the *trans* position by two oxygen atoms of the ligand. This crystallographic environment appears as a coordination sphere satisfying the more stable positioning of the both atoms of oxygen and nitrogen in phenoxy and azomethine groups of the Schiff base ligand [**Ni:** O3, O3i, N2, N2i (i:-x–y-z)]. The azomethine linkage is evident from the N2–C7 bond length which is equal 1.289 Å very close to the typical bond length (1.29–1.32 Å) in imines. As for the C7–N2–C8 angle, it is equal to 114.1° (Allen et al. 1987). The bond lengths involving the phenyl ring and phenoxy oxygen atoms, C4–O3 and C15–O4, are 1.383 and 1.372 Å, respectively, and these values are seen in the range of the usually observed standard C(sp^2)–OH and C(sp^2)–O– bond length (Kwiatkowski et al. 1990). The Ni–O and Ni–N bond lengths for **Ni(II)-2L** varying in the range 1.821–1.831 Å and 1.918–1.919 Å, respectively, and are in good agreement with related reported complexes (Bhowmik et al. 2011). Cisoid and transoid angles of the nickel deviate from their ideal values of 90° and 180° and found to be in the ranges 86.3°–93.1° and 178.2°–176.5°, respectively. The bond length and angle around C16 (methoxy atom) are consistent with sp^3 hybridizations of this atom (Ourari et al. 2013).

The crystal packing for **Ni(II)-2L** can be described as alternating layers parallel to (101) plane (Fig. 5), and molecules are also linked via C–H–O intermolecular hydrogen bonds forming an infinite two-dimensional network in one layer (Fig. 6, Table 4).

The crystal structure is also supported by intermolecular interactions of Cg–Cg ($\pi - \pi$ stacking) interactions between aromatic rings. The shortest centroid–centroid distance is estimated to 3.6266 (1) Å. All these interactions link the molecule within the layers and also link their layers together by reinforcing the cohesion of the structure.

Cyclic voltammetry of the Ni(II)-2L

The electrochemical behavior of the nickel(II) complex was studied in DMF solutions containing 10^{-1}M tetra(n-butyl)ammonium perchlorate (TBAP). This medium is used because the radical anions of aromatic nitro-compounds are more stable in aprotic solvents such as DMF (Grimshaw 2000; Toro et al. 2018). The nickel(II) complex showed voltammetric responses in the cathodic and anodic regions where the reduction and oxidation waves were observed at $Ep_{c2} = -1.51$ and $Ep_{a2} = -1.39$ V versus SCE, respectively. These waves are ascribed to the Ni(II)/Ni(I) redox system (Ourari and Aggoun 2015). The voltammetric data of nickel(II) complex were recorded using various scan rates in the potential values ranging of -1.0 and -1.8 V versus SCE. These electrochemical characteristics are summarized in Table 5 and displayed in Fig. 7.

The effect of the scan rate on the voltammetric responses of the synthesized complex was also analyzed (Fig. 7b). As it can be seen, the peak currents increase with the increase in the square root of scan rates and vary linearly indicating the diffusion redox process (Figure 7c, d). Table 5 shows the electrochemical parameters obtained from the voltammograms, and it can be observed that the potential peak-to-peak separation appeared around 59 and 100 mV. According to these results, it can be deduced that the redox couple was related to a quasi-reversible expressing a monoelectronic transfer process, controlled by diffusion (Ourari et al. 2017, 2018).

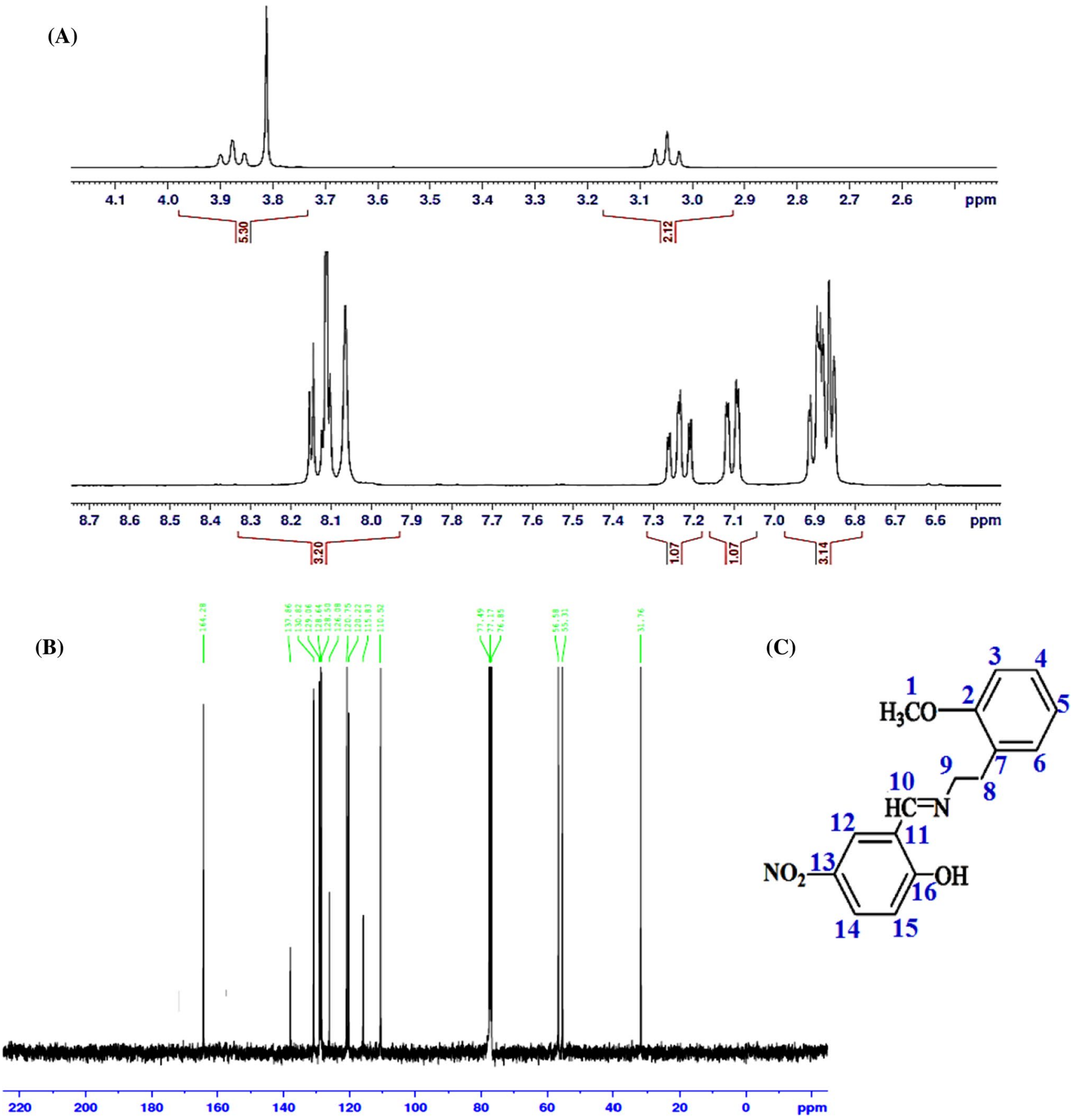

Fig. 3 **a** ^{1}H NMR, **b** ^{13}C NMR spectra of the Schiff base **HL** and **c** molecular structure of the Schiff base **HL** as deduced from A) and B)

Antioxidant activity

The free radical scavenging ability of the synthesized compounds was determined by useful method of DPPH, in which the reduction of this radical in presence of antioxidant agent led to a solution color changing from the purple to yellowish. In this study, our results depicted in Fig. 8a indicate that the scavenging effect is concentration dependent of the tested compounds. From these results, the complex **Ni(II)-2L** exhibited an efficient effect with an inhibition percentage of 68.47% followed by the ligand **HL** presenting an inhibition percentage of 59.57%. As for the potential effect determination, we have used the IC$_{50}$ values which seem to be more significant. Our findings are displayed in Fig. 8b and demonstrate that the **Ni(II)-2L** complex has the highest scavenging effect with its lower IC$_{50}$ value estimated

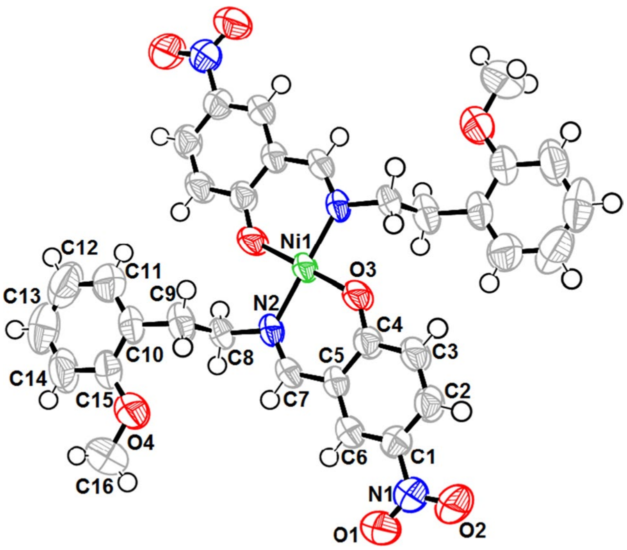

Fig. 4 The molecular geometry of compound **Ni(II)-2L**. No labeled atoms are generated by inversion center symmetry ($-x, -y, -z$). Displacement ellipsoids are drawn at the 50% probability level. H atoms are represented as small spheres of arbitrary radius

to 0.42 mg/mL, whereas the IC_{50} value of the ligand **HL** was found to be 4.51 mg/mL. These results revealed that they are in good accordance with previous similar studies reported in the literature (Pramanik et al. 2015; Jamil et al. 2019; Charef et al. 2015). In this case, it was concluded that the metal complexes were found be more active than their ligands themselves.

Conclusion

In this paper, we have presented the synthesis of a bidentate Schiff base ligand (**HL**) and its new nickel(II)–Schiff base complex (**Ni(II)-2L**). These two compounds have been thoroughly characterized by conventional spectroscopic techniques, such as IR, UV–Vis, ^{1}H- and ^{13}C-NMR, and elemental analysis. This structural characterization was supported by XRD diffraction analysis of our nickel complex. The results of these analyses, including the crystallographic studies, have as main goal to elucidate the molecular structures of the synthesized compounds like the nickel complex and its ligand. In comparison with ascorbic acid as a standard, these compounds revealed to have a respectable inhibition activity toward a free radical scavenging capacity assayed by DPPH free radical method. It was found that the IC_{50} value of the nickel complex is lower than those of its corresponding Schiff base ligand. The electrochemical behavior of the nickel complex has also been investigated. In this case, we have found that the relationship between the anodic peak current (ip_a) and the square root of scan rate ($v^{1/2}$) is linear, suggesting that the electrochemical process is mainly governed by diffusion.

Table 3 Crystal data, data collection and structure refinement parameters for and **Ni(II)-2L**

Compound	**Ni(II)-2L**
Empirical formula	C_{32} H_{30} N_4 Ni O_8
Formula weight	657.31
T (K)	150
λ (Å)	0.71073
Crystal system	Triclinic
Space group	P-1
a(Å), b(Å), c(Å)	6.6803 (2), 9.6702 (2), 12.1836 (3)
(°)α, (°)β, (°)γ	109.305 (1), 93.442 (1), 102.281 (1)
V (Å^3), Z	718.52 (3), 1
ρ (g cm^{-3})	1.519
μ (mm^{-1})	0.737
F (000)	342.0
Limiting indices	h:− 6/8, k:− 12/12, l: − 16/16
Data/restraints/	3523
Parameters	206
Total reflections	12,833
Unique reflections (Rint)	3523 (0.0292)
Refinement method	Full least-squared (Shelxl-97)
Goodness of fit on F^2	1.048
Final R index [$I > 2\sigma(I)$]	0.0322
R index [all data]	0.0401
Largest difference peak and hole (e Å^{-3})	0.284/− 0.262
CCDC deposition no.	CCDC1912564

$R = \{\sum[w(|F_o| - |F_c|)]/\sum w(|F_o|)\}$, $Rw = \{\sum w(|F_o| - |F_c|)^2]/\sum w(|F_o|^2)\}^{1/2}$

$wR2 = \{\sum[w(F_o^2 - F_c^2)^2]/\sum w(F_o^2)\}^{1/2}$

$w = 1/\sigma^2(F_0^2) + (0.0794P)^2 + 0.6853P]$ where $P = (F_o^2 + 2F_c^2)/3$

Supplementary data

Crystallographic data have been deposited at the Cambridge Crystallographic Data Centre. CCDC 1912564 contains the supplementary crystallographic data for **Ni(II)-2L**. These data can be obtained free of charge via http://www.ccdc.cam.ac.uk/conts/retrieving. html, or from the CCDC, 12 Union Road, Cambridge, CB2 1EZ, UK; fax: (+44) 01223-336-033; e-mail: deposit@ccdc.cam.ac.

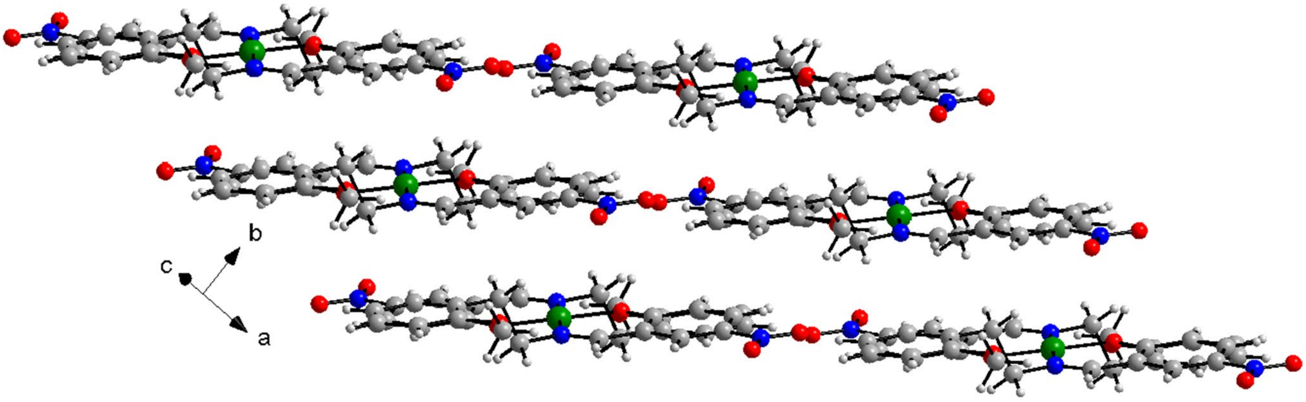

Fig. 5 Diagram packing of **Ni(II)-2L**, showing an alternating parallel layers to (101) plane

Fig. 6 Interactions of C–H–O (dashed line in blue) hydrogen bonding, resulting in the formation of an infinite two-dimensional network in one layer

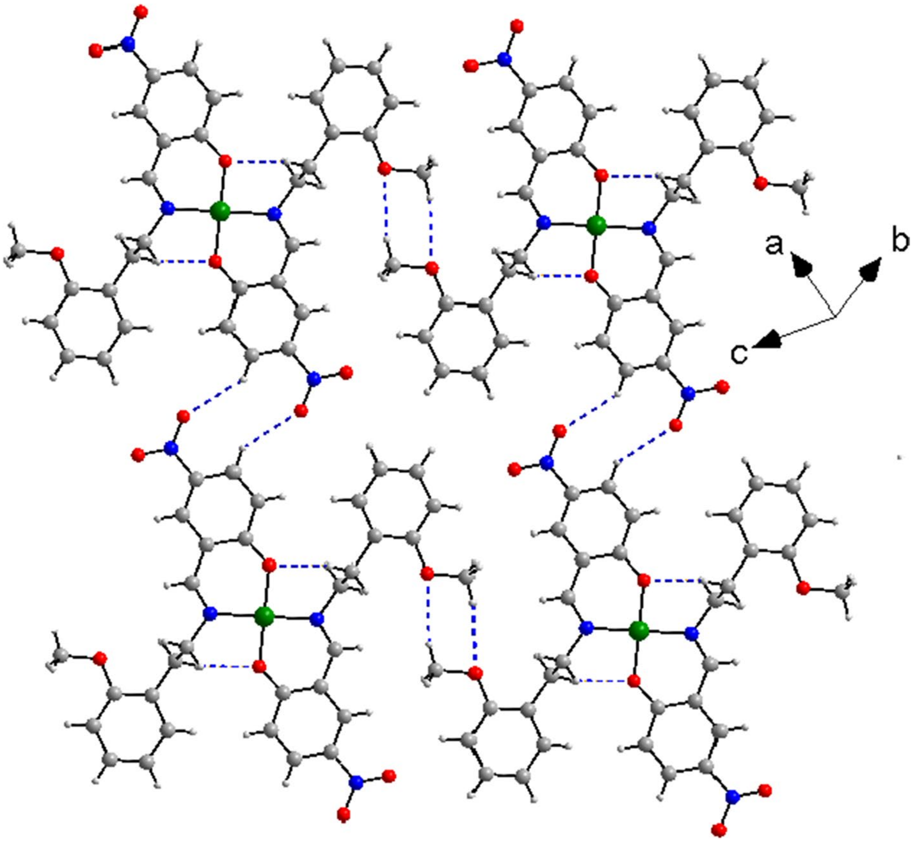

Table 4 Distances (Å) and angles (°) of hydrogen bond for **Ni(II)-2L**

D–H–A	*d* (D–H)	*d*(H–A)	*d* (D–A)	D–H–A	Symmetry
C8–H8a–O3	0.97	2.24	2.6923 (1)	107.0	$-x, -y+1, -z$
C16–H16b–O4	0. 94	2.58	3.5055 (1)	161.0	$-x+1, -y+1, -z+1$

Table 5 Cyclic voltammetric parameters of the nickel complex with various scan rates

v (mV s^{-1})	Ip_{a2} (μA/cm^2)	Ip_{c2} (μA/cm^2)	Ep_{a2} (V)	Ep_{c2} (V)	$E_{1/2}$ (V)	ΔE (V)	*ipa/ipc*
25	3.686	6.485	−1.352	−1.472	−1.412	0.060	0.568
50	4.655	8.321	−1.339	−1.478	−1.408	0.069	0.559
75	5.395	9.638	−1.339	−1.483	−1.411	0.072	0.559
100	5.160	10.445	−1.355	−1.480	−1.417	0.062	0.494
200	6.537	13.517	−1.341	−1.486	−1.413	0.072	0.483
300	7.308	15.793	−1.328	−1.494	−1.415	0.087	0.462
400	8.422	17.204	−1.320	−1.499	−1.409	0.089	0.489
500	10.076	17.390	−1.298	−1.542	−1.445	0.097	0.579

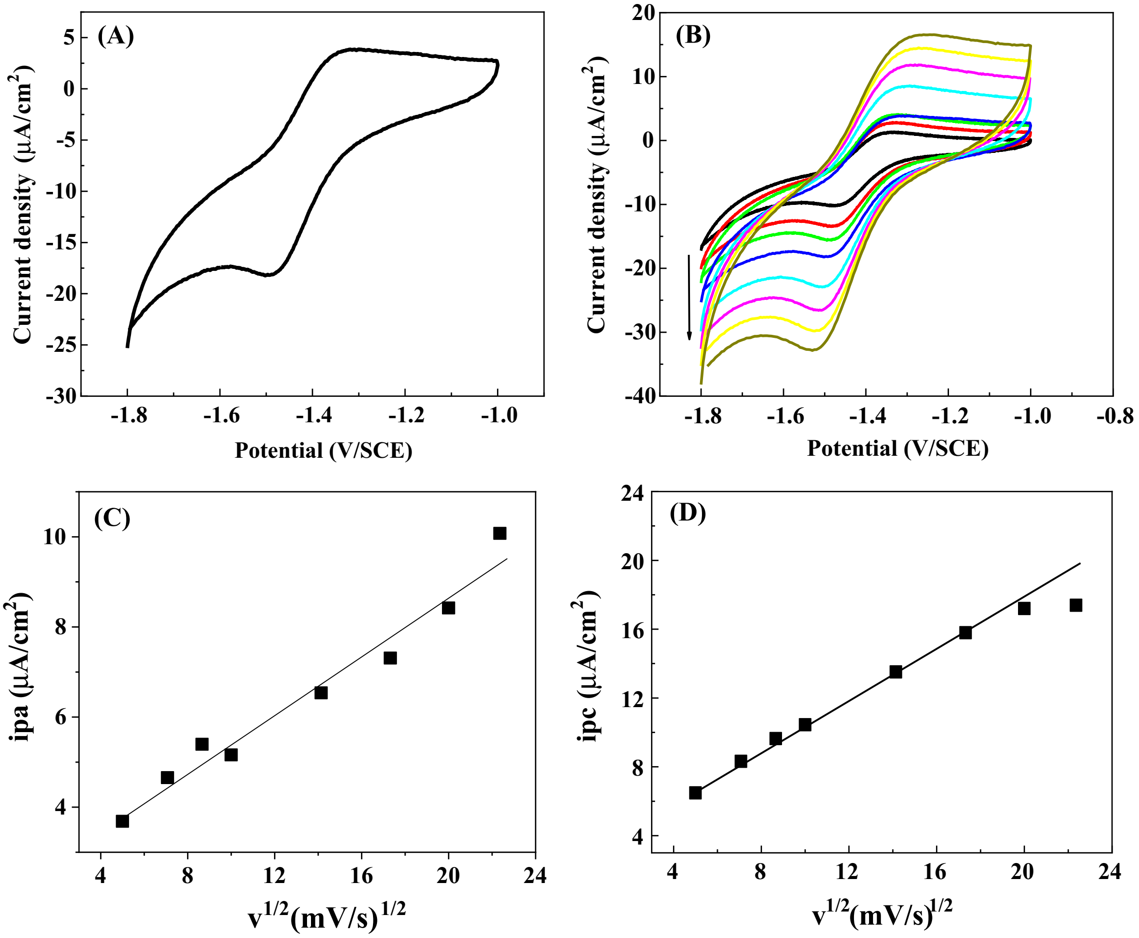

Fig. 7 **a** Cyclic voltammograms of the synthesized complex of **Ni(II)-2L** showing the response of **Ni(II)/Ni(I)** redox couple, recorded in 0.1 mol L^{-1} TBAP/DMF solution at 298 K at 100 mVs^{-1}; **b** cyclic voltammograms of nickel complex in 0.1 M TBAP/DMF solutions, recorded at various scan rates: from inner to outer, 25, 50, 75, 100, 200, 300, 400 and 500 (mVs^{-1}), respectively. The anodic **(c)** and cathodic **(d)** currents versus square root scan rate (v$^{1/2}$)

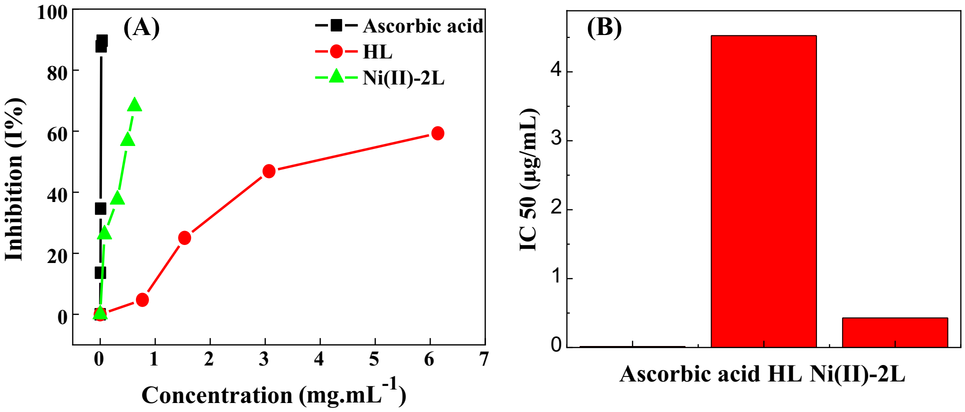

Fig. 8 **a** DPPH radical scavenging activity of the ligand (**HL**) and its Ni(II) complex (**Ni(II)-2L**), compared to the ascorbic acid used as standard reference; **b** IC_{50} inhibitory concentration of ligand and nickel complex for 50% of DPPH radical. Comparison was made against ascorbic acid

Acknowledgements The authors thank the Algerian Ministry of Higher Education and Scientific Research (MESRS) and the Directorate General of Scientific Research and Technological Development (DGRSDT) for their financial support. The authors also gratefully acknowledge the financial help (MAT2016-76595-R) of the Ministerio de Economía y Competitividad and FEDER. Special thanks are owed to the Spanish Ministry of Economy and Competitiveness (MINECO) for the granting of a “Ramón y Cajal” contract (RYC-2017-23618).

References

Al Zoubi W, Al-Hamdani AAS, Kaseem M (2016) Synthesis and antioxidant activities of Schiff bases and their complexes: a review. Appl Organometal Chem 30:810–817. https://doi.org/10.1002/aoc.3506

Al-allaf TAK, Sheet AZM (1995) Platinum group metal Schiff base complexes-I. Platinum complexes. Polyhedron 14:239–248. https://doi.org/10.1016/0277-5387(94)00231-3

Allen FH, Kennard O, Watson DG, Brammer L, Orpen AG, Taylor R (1987) Tables of bond lengths determined by X-ray and neutron diffraction. Part 1. Bond lengths in organic compounds. J Chem Soc Perkin Trans 12:S1–S19. https://doi.org/10.1039/p298700000s1

Altun Y, Köseoğlu F, Demirelli H, Yılmaz İ, Çukuroval A, Kavak N (2009) Potentiometric studies on nickel(II), copper(II) and zinc(II) metal complexes with new schiff bases containing cyclobutane and thiazole groups in 60% dioxane-water mixture. J Braz Chem Soc 20:299–308. https://doi.org/10.1590/S0103-50532009000200015

Alturk S, Tamer O, Avci D, Atalay Y (2015) Synthesis, spectroscopic characterization, second and third-order nonlinear optical properties, and DFT calculations of a novel Mn(II) complex. J Organomet Chim 797:110–119. https://doi.org/10.1016/j.jorganchem.2015.08.014

Amirnasr M, Schenk KJ, Gorji A, Vafazadef R (2001) Synthesis and spectroscopic characterization of $[Co^{III}(salophen)(amine)_2]ClO_4$(amine = morpholine, pyrrolidine, and piperidine) complexes. The crystal structures of $[Co^{III}(salophen)(morpholine)_2]ClO_4$ and $[Co^{III}(salophen)(pyrrolidine)_2]ClO_4$. Polyhedron 20:695–702. https://doi.org/10.1016/S0378-3758(01)00095-7

Bedioui F, Labbe E, Gutierrez-Granados S, Devynck J (1991) Electrooxidative polymerization of cobalt, nickel and manganese salen complexes in acetonitrile solution. J Electroanal Chem 301:267–274. https://doi.org/10.1016/0022-0728(91)85477-7

Bhattacharya P, Parr J, Ross AT (1998) First synthesis of a unique dilead Schiff base complex. J Chem Soc Dalton 19:3149–3150. https://doi.org/10.1039/a806058d

Bhowmik P, Drew MGB, Chattopadhyay S (2011) Synthesis and characterization of nickel(II) and copper(II) complexes with tetradentate Schiff base ligands. Inorg Chim Acta 366:62–67. https://doi.org/10.1016/j.ica.2010.10.010

Brandenburg K, Berndt M (2001) DIAMOND. Crystal Impact, Bonn

Burla MC, Caliandro R, Camalli M, Carrozzini B, Cascarano GL, De Caro L, Giacovazzo C, Polidori G, Spagna R (2005) SIR2004: an improved tool for crystal structure determination and refinement. J Appl Cryst 38:381–388. https://doi.org/10.1107/S002188980403225XU

Chang H-Q, Jia L, Xu J, Zhu T-F, Xu Z-Q, Chen R-H, Ma T-L, Wang Y, Wu W-N (2016) Syntheses, crystal structures, anticancer activities of three reduce Schiff base ligand based transition metal complexes. J Mol Struct 1106:366–372. https://doi.org/10.1016/j.molstruc.2015.11.001

Charef N, Sebti F, Arrar L, Djarmouni M, Boussoualim N, Baghiani A, Khennouf S, Ourari A, Al Damen MA, Mubarak MS, Peters DG (2015) Synthesis, characterization, X-ray structures, and biological activity of some metal complexes of the Schiff base 2,20-(((azanediylbis(propane-3,1-diyl))bis(azanylylidene))bis(methanylylidene))diphenol. Polyhedron 85(2015):450–456. https://doi.org/10.1016/j.poly.2014.09.006

Cisterna J, Dorcet V, Manzur C, Ledoux-Rak I, Hamon J-R, Carrillo D (2015) Synthesis, spectral, electrochemical, crystal structures and nonlinear optical properties of unsymmetrical Ni(II) and Cu(II) Schiff base complexes. Inorg Chim Acta 430:82–90. https://doi.org/10.1016/j.ica.2015.02.030

Dalia SA, Afsan F, Hossain MS, Khan MN, Zakaria CM, Kudrat-E-Zahanand M, Ali MM (2018) A short review on chemistry of schiff base metal complexes and their catalytic application. Int J Chem Stud 6:2859–2866. https://doi.org/10.22271/chemi

Das A, Trousdale MD, Ren S, Lien E (1999) Inhibition of herpes simplex virus type 1 and adenovirus type 5 by heterocyclic Schiff bases of aminohydroxyguanidinetosylate. J Antiviral Res 44:201–208. https://doi.org/10.1016/s0166-3542(99)00070-4

Dey M, Rao CP, Saarenketo PK, Rissanen K (2002) Mono-, di- and tri-nuclear Ni(II) complexes of N-, O-donor ligands: structural diversity and reactivity. Inorg Chem Commun 5:924–928. https://doi.org/10.1016/S1387-7003(02)00602-0

Dey M, Rao CP, Saarenketo PK, Rissanen K, Kolehmainen E, Guionneau P (2003) Mn(IV) and Co(III)-complexes of –OH- rich ligands possessing O_2N, O_3N and O_4N cores: syntheses, characterization and crystal structures. Polyhedron 22:3515–3521. https://doi.org/10.1016/j.poly.2003.09.015

Djebbar SS, Benali BO, Deloume JP (1997) Synthesis, characterization and electrochemical behaviour of some copper(II) complexes with linear and tripodal tetradentate ligands derived from Schiff bases. Polyhedron 16:2175–2182. https://doi.org/10.1080/00945719708000259

Djebbar SS, Benali BO, Deloume JP (1998) Synthesis, characterization, electrochemical behavior and catalytic activity of manganese(II) complexes with linear and tripodal tetradentate ligands derived from Schiff bases. Transit Met Chem 23:443–447. https://doi.org/10.1023/A:1006945006419

Ebrahimi HP, Hadi JS, Abdulnabi ZA, Bolandnazar Z (2014) Spectroscopic, thermal analysis and DFT computational studies of salen-type Schiff base complexes. Spectrochim Acta A 117:485–492. https://doi.org/10.1016/j.saa.2013.08.044

El-Megharbel SM, Megahed AS, Refat MS (2016) Preparation, physical and chemical studies on metal complexes of Schiff bases as a nucleus key to prepare nanometer oxides have catalytic applications: nickel(II) complexes derived from 4-aminoantipyrine derivatives. J Mol Liq 216:608–614. https://doi.org/10.1016/j.molliq.2016.01.097

Farrugia LJ (1997) ORTEP-3 for windows: a version of ORTEP-III with a graphical user interface (GUI). J Appl Cryst 30:565. https://doi.org/10.1107/S0021889897003117

Farrugia LJ (2012) WinGX and ORTEP for windows: an update. J Appl Cryst 45:849–854. https://doi.org/10.1107/S0021889812029111

Gorczyński A, Pakulski D, Szymańska M, Kubicki M, Bułat K, Łuczak T, Patroniak V (2016) Electrochemical deposition of the new manganese(II) Schiff-base complex on a gold template and its application for dopamine sensing in the presence of interfering biogenic compounds. Talanta 149:347–355. https://doi.org/10.1016/j.talanta.2015.11.050

Grimshaw J (2000) Electrochemical reactions and mechanisms in organic chemistry. Elsevier. ISBN: 978-0-444-72007-8

Gungor E, Kara H (2011) A new hydrogen-bonded pseudo-dimer Mn(III) Schiff base complex: the synthesis, X-ray structure and spectroscopic studies. Spectrochim Acta A 82:217–220. https://doi.org/10.1016/j.saa.2011.07.038

Highfield JA, Mehta LK, Parrick J, Wardman P (2000) Synthesis, hydroxyl radical production and cytotoxicity of analogues of bleomycin. Bioorg Med Chem 8:1065–1073. https://doi.org/10.1016/s0968-0896(00)00042-0

Hopa C, Kurtaran R, Alkan M, Kara H, Hughes R (2010) Synthesis, characterization and thermal properties of cobalt(II), nickel(II) and copper(II) complexes of 2,6-bis(3,4,5-trimethyl-N pyrazolyl)pyridine): the crystal structure of [Co(btmpp)$(H_2O)_2(NO_3)]NO_3$. Transit Met Chem 35:1013–1018. https://doi.org/10.1007/s11243-010-9424-4

Ilhan S, Temel H, Kılıc A, Yılmaz I (2007) Synthesis, characterization and redox properties of macrocyclic Schiff base by reaction of 2,6-diaminopyridine and 1,3-bis(2-carboxyaldehyde phenoxy)propane and its Cu^{II}, Ni^{II}, Pb^{II}, Co^{III} and La^{III} complexes. Transit Met Chem 32:344–349. https://doi.org/10.1007/s11243-006-0174-2

Jamil W, Solangi S, Ali M, Khan KM, Taha M, Khuhawar MY (2019) Syntheses, characterization, in vitro antiglycation and DPPH radical scavenging activities of isatin salicylhydrazidehydrazone and its Mn(II), Co(II), Ni(II), Cu(II), and Zn(II) metal complexes. Arab J Chem 12:2262–2269. https://doi.org/10.1016/j.arabjc.2015.02.015

Kara H, Naturforsch Z (2008) A dimeric Mn(III) complex of a quadridentate Schiff base ligand, synthesis, structure and ferromagnetic exchange. Zeitschrift fur Naturforschung B 63b:6–10. https://doi.org/10.1515/znb-2008-0102

Keypour H, Shayesteh M, Rezaeivala M, Chalabian F, Valencia L (2013) Synthesis and characterization of a series of transition metal complexes with a new symmetrical polyoxaazamacroacyclic Schiff base ligand: x-ray crystal structure of cobalt(II) and nickel(II) complexes and their antibacterial properties. Spectrochim Acta A 101:59–66. https://doi.org/10.1016/j.saa.2012.09.048

Khalaji AD, Rad SM, Grivani G, Das D (2011) Nickel(II) and copper(II) complexes with an asymmetric bidentate Schiff-base ligand derived from furfurylamine: synthesis, spectral, XRD, and thermal studies. J Therm Anal Calorim 103:747–751. https://doi.org/10.1007/s10973-010-1024-1

Kuchtanin V, Kleščíková L, Šoral M, Fischer R, Růžičková Z, Rakovský E, Moncoľ J, Segľa P (2016) Nickel(II) Schiff base complexes: synthesis, characterization and catalytic activity in Kumada-Corriu cross-coupling reactions. Polyhedron 117:90–96. https://doi.org/10.1016/j.poly.2016.05.037

Kwiatkowski M, Kwiatkowski E, Olechnowicz A, Ho DM, Deutsch E (1990) New nickel(II) and palladium(II) complexes with unsymmetrical quadridentate Schiff bases derived from 8-amino-4-methyl-5-azaoct-3-en-2-one. Crystal and molecular structure of [4,10-dimethyl-3-(nitroso-χN)-5,9-(diaza-χ2N)-trideca-3,10-diene-2,12-(dionato-χO)(2–)]nickel(II). J Chem Soc, Dalton Trans 8(1990):2497–2502. https://doi.org/10.1039/dt9900002497

Luca OR, Blakemore JD, Konezny SJ, Praetorius JM, Schmeier TJ, Hunsinger GB, Batista VS, Brudvig GW, Hazari N, Crabtree RH (2012) Organometallic Ni pincer complexes for the electrocatalytic production of hydrogen. Inorg Chem 51:8704–8709. https://doi.org/10.1021/ic300009a

Nassimbeni LR, Percy GC, Rodgers AL (1976) The crystal and molecular structure of hexaaquacobalt(II) bis(N-salicylideneglycinato)cobaltate(III) dihydrate. Acta Crystallogr Sect B Struct Crystallogr Cryst Chem 32:1252–1256. https://doi.org/10.1107/S0567740876005050

Odabasioglu S, Kurtaran R, Azizoglu A, Kara H, Sevi O, Atakol O (2009) Experimental and computational study on [2, 6-bis (3, 5-dimethyl-N-pyrazolyl) pyridine]-(dithiocyanato) mercury (II). Cent Eur J Chem 7:402–409. https://doi.org/10.2478/s11532-009-0027-x

Ourari A, Aggoun D (2015) Synthesis and spectral analysis of N-substituted pyrrole salicylaldehyde derivatives-electropolymerization of a new nickel(II)-Schiff base complex derived from 6-[3′-*N*-pyrrolpropoxy]-2-hydroxyacetophenone and 1,2-diaminoethane. J Iran Chem Soc 12:1893–1904. https://doi.org/10.1007/s13738-015-0664-2

Ourari A, Aggoun D, Ouahab L (2013) A novel copper(II)-Schiff base complex containing pyrrole ring: synthesis, characterization and its modified electrodes applied in oxidation of aliphatic alcohols. Inorg Chem Commun 33:118–124. https://doi.org/10.1016/j.inoche.2013.04.002

Ourari A, Ouennoughi Y, Aggoun D, Mubarak MS, Pasciak EM, Peters DG (2014) Synthesis, characterization, and electrochemical study of a new tetradentate nickel(II)-Schiff base complex derived from ethylenediamine and 5′-(N-methyl-N-phenylaminomethyl)-2′-hydroxyacetophenone. Polyhedron 67:59–64. https://doi.org/10.1016/j.poly.2013.08.056

Ourari A, Bougossa I, Bouacida S, Aggoun D, Ruiz-Rosas R, Morallon E, Merazig H (2017) Synthesis, characterization and X-ray crystal structure of novel nickel Schiff base complexes and investigation of their catalytic activity in the electrocatalytic reduction of alkyl and aryl halides. J Iran Chem Soc 14:703–715. https://doi.org/10.1007/s13738-016-1022-8

Ourari A, Alouache A, Aggoun D, Ruiz-Rosas R, Morallon E (2018) Electrocatalytical reduction of bromocyclopentane and iodobenzene using Cobalt(III) and Nickel(II) Tris- and Bis-bidentates Schiff Bases Complexes. Int J Electrochem Sci 13:5589–5602. https://doi.org/10.20964/2018.06.39

Pooyan M, Ghaffari A, Behzad M, Rudbari HA, Bruno G (2013) Tetradentate N_2O_2 type Nickel(II) Schiff base complexes derived from meso-1,2-diphenyle-1,2-ethylenediamine: synthesis, characterization, crystal structures, electrochemistry, and catalytic studies. J Coord Chem 66:4255–4267. https://doi.org/10.1080/00958972.2013.867031

Pramanik HAR, Paul PC, Mondal P, Bhattacharjee CR (2015) Mixed ligand complexes of cobalt(III) and iron(III) containing N_2O_2-chelating Schiff base: synthesis, characterization, antimicrobial activity, antioxidant and DFT study. J Mol Struct 1100:496–505. https://doi.org/10.1016/j.molstruc.2015.07.076

Sheldrick GM (2008) A short history of SHELX. Acta Cryst A 64:112–122. https://doi.org/10.1107/S0108767307043930

Tai X, Yin X, Chen Q, Tan M (2003) Synthesis of some transition metal complexes of a novel Schiff base ligand derived from 2,2′-bis(p-Methoxyphenylamine) and salicylicaldehyde. Molecules 8:439–443. https://doi.org/10.3390/80500439

Toro P, Suazo C, Acuňa A, Fuentealba M, Artigas V, Arancibia R, Olea-Azar C, Moncada M, Wilkinson S, Klahn AH (2018) Cyrhetrenylaniline and new organometallic phenylimines derived from 4- and 5-nitrothiophene: synthesis, characterization, X-Ray structures, electrochemistry and in vitro anti-T. brucei activity. J Organomet Chem 862:13–21. https://doi.org/10.1016/j.jorganchem.2018.03.004

VimalKumar PM, Radhakrishnan PK (2011) Synthesis, spectral and X-ray structural studies of a NO donor Schiff base ligand and its Ni(II) complexes. Inorg Chim Acta 375:84–92. https://doi.org/10.1016/j.ica.2011.04.034

Wu JC, Tang N, Liu WS, Tan MY, Chan ASC (2001) Intramolecular hydrogen bond self-template synthesis of some new Robson-type macrocyclic ligands. Chin Chem Lett 12:757–760

Yahsi Y, Kara H, Sorace L, Buyukgungor O (2011) Mono-and dinuclear Fe(III) complexes with the N_2O_2 donor 5-chlorosalicylideneimine ligands;synthesis, X-ray structural characterization and magnetic properties. Inorg Chem Acta 366:191–197. https://doi.org/10.1016/j.ica.2010.10.027